

05

Critical current in a long Josephson contact with weak pinning in an external magnetic field

© M.A. Zelikman

Peter the Great Saint-Petersburg Polytechnic University,
195251 St. Petersburg, Russia
e-mail: marzelik@mail.ru

Received November 3, 2021

Revised December 14, 2021

Accepted December 15, 2021

The analysis of possible current distributions when passing current through a periodically modulated long Josephson contact located in an external magnetic field is carried out. An approach based on the analysis of continuous configuration modification proceeding in the direction of Gibbs potential reduction is used for the calculation. The case when the pinning parameter is less than the critical value is considered. It is shown that at any value of the external magnetic field, there is a critical value of the transport current, when exceeded, the situation ceases to be stationary, as a result of which energy passes into radiation and heat, i.e. currents cease to be persistent. The value of the critical current is determined by the value of the magnetic field at which the vortices begin to fill the entire length of the contact. With an increase in the external magnetic field, the critical value of the current decreases.

Keywords: high-temperature superconductors, pinning, Josephson contacts.

DOI: 10.21883/TP.2022.03.53263.285-21

Introduction

Over the last years the series of theoretical and experimental studies were performed, that bring us closer to superconductivity at room temperature [1,2]. Therefore, the problem of critical fields and currents became even more important for practical use of superconductors. This problem is solved in the low-temperature superconductors based on Ginzburg-Landau theory. High-temperature superconductors (HTSC) are mainly ceramics, consisting of contacting granules separated with dielectric. In the places of the granules contact the Josephson contacts appear, that are described with non-linear equations, thus complicating the theoretical analysis. Porosity of the ceramic HTSC, resulting in samples inhomogeneity and vortices pinning, also raises difficulties. This prevents from Ginzburg-Landau equations using for calculation of current states in HTSC. Other approaches to analysis of phenomena in such media should be searched.

Over the last years the interest of physicists, studying the superconductivity, was focused on Josephson junctions. On the one hand, structures of this type can be made artificially [3,4]. Processes in the long Josephson contacts attract attention, for instance, regarding the idea of short contacts chain using for radiation efficiency increase [5]. Long contacts, in which dielectric in a layer between the superconductors is replaced with ferromagnetic, are also studied [6]. On the other hand, such contact is a model, applicable to all processes in the superconducting samples: Meissner state, vortices existence, their pinning and all

related phenomena. In this model the calculations can be performed extremely accurate, that allows to understand the occurring processes in detail. Therefore, the processes in the long Josephson contacts are analyzed in a lot of the works [7–9].

The artificial periodically modulated Josephson contact (Fig. 1, *a*) is a thin layer of dielectric (xz plane) between two superconductors, crossed with parallel with each other and infinite along z axis dielectric strips with thickness l along y axis and width d along x axis, periodically located along x axis at distance L from each other. The external magnetic field, as well as vortices axes are directed along z axis. Fig. 1, *b* shows the structure of artificially created periodically modulated Josephson contact [3]. On the sections between the strips the value of phase jump between the contact sides slowly changes with coordinate, while at junction through the strip it changes abruptly. Let's indicate the jump value, averaged over k -th section between the strips, through φ_k (Fig. 1, *a*). Let's assume, that the phase jump at the section, closest to the contact boundary, is equal to φ_1 , and φ_2, φ_3 , etc with movement inward. Distribution of values of φ_k describes the steady current state.

In the works [10–12] it was shown, that contact behavior in the magnetic field is defined with the value of so called pinning parameter $g = 2\pi\mu_0 i_C L d / \Phi_0$ (in [10,11] designation I is used). Here, i_C is critical current density of each point Josephson junction, Φ_0 is magnetic flux quantum, meaning of values L, l, d is clear from Fig. 1. At low values of g situation is the same as at zero pinning, i.e. when the external field exceeds some value of H_{\max} the vortices fill the whole contact at once —

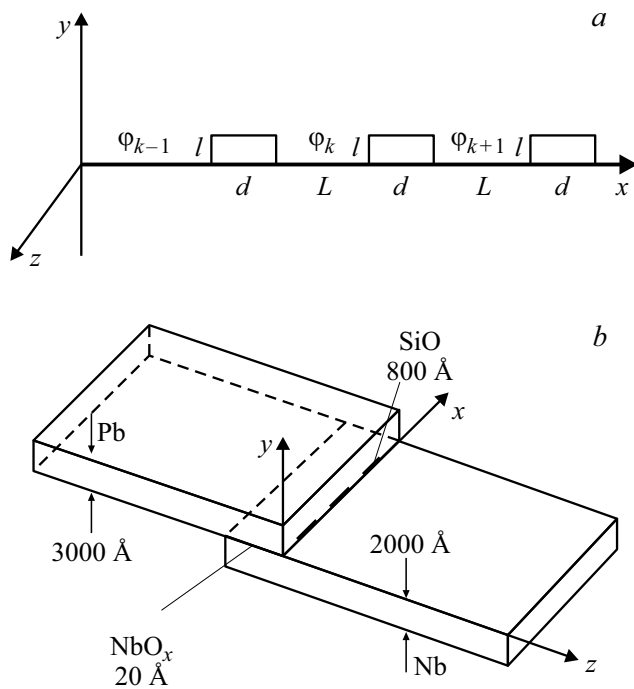


Figure 1. *a* — model of periodically modulated Josephson contact; *b* — structure of artificially created periodically modulated Josephson contact.

from its boundary to infinity. This is similar to situation in the II-type superconductor. At higher values of g the vortices, with field growth, gradually move from the boundary to the interior of the contact, while the magnetic field in the contact depth remains equal to zero, i.e. the situation is similar in the III-type superconductor. In [11] it is shown, that these two modes are divided with the critical value of pinning parameter g_C , that which is within a range of 0.95–1.00. In [12] based on approach, developed in non-linear physics [13], the exact value is found $g_C = 0.9716$. At $g > g_C$ there is a possibility of unlimited growth of the field towards the contact boundary, i.e. at any external field the finite length current configuration can exist near the boundary, providing the complete field compensation inside the contact far from the boundary.

In the work [11] the long contact in the external magnetic field is examined, when the total current through the contact is equal to zero. In the work [12] the currents distribution in the contact at specified total current in zero external magnetic field is calculated. In the work [14] the analysis of the general case, when both current and external magnetic field are not equal to zero, is performed at pinning parameter values, exceeding the critical value ($g > g_C$).

The purpose of this work is a detailed study of the general case at $g < g_C$, when the long Josephson contact is put into the external magnetic field, and through this contact the persistent superconducting current is flowing.

1. Problem statement and calculation technique

If there is the pinning, the distribution of phase jumps and currents over the contact is not unambiguous. The reason behind that is a „hysteresis nature“ of the situation: type of the settled configuration depends on prehistory, i.e. how this state was set. For instance, if firstly we put the contact in any small field and then we cool it and transfer into the superconducting state, the magnetic flux will also penetrate the internal cells of the contact. If we put it into the field in superconducting state, then at low fields the configuration will be of Meissner type, i.e. the field penetrates only narrow layer near the boundary. There are a lot of options. Let's solve this problem for the case of gradual field inclusion and the following increase of transport current. The contact is in superconducting state already, while the external field slowly increases from zero value to H_e . After that the external current is passed through the contact, and this current slowly and monotonously increases from zero to J . Let's introduce the dimensionless parameters

$$h = H_e/H_0, \quad j = J/bH_0,$$

where $H_0 = \Phi_0/\mu_0 S$ is value of external field, at which 1 quantum of magnetic flux Φ_0 is passed through the cell with area S , b is contact length along z axis (Fig. 1).

Let's assume that the external field \mathbf{H}_e is directed against us (against z axis in Fig. 1), while transport current — upward (along y axis). Then, the total field outside of contact from the right side is equal to $h + j/2$, while from the left side — $h - j/2$.

Let's apply the method, used in [11] for calculation of the field profile in the contact at zero total current. At the first stage we will consider the total current as equal to zero and find the field profile in the contact at monotonous increase of the external field H_e .

Let's examine the finite length contact, containing an odd number of cells $2N - 1$, i.e. number of current series is equal to $2N$. Let's write the Gibbs potential of such configuration with a height of 1 m [2]

$$G = E - \int BHdV = \frac{\Phi_0^2}{2\pi^2\mu_0 S} \sum_{i=1}^{2N-1} \left[\left(\frac{1}{2}(\varphi_{i+1} - \varphi_i)^2 + g(1 - \cos \varphi_i) \right) - 2\pi h(\varphi_1 - \varphi_{N+1}) \right]. \quad (1)$$

For definiteness we assume that $i = 1$ in the extreme left row. At conclusion (1) we considered, that in the examined geometry the thermodynamic intensity of the magnetic field H in all points is the same and equal to the intensity of the external field H_e , and we used the conditions of fluxoid quantization

$$2\pi\Phi_m/\Phi_0 + \varphi_m - \varphi_{m+1} = 0, \quad (2)$$

where Φ_m is total magnetic flux through m -th cell. Then,

$$\begin{aligned} \int BHdV &= H_e \sum_i \Phi_i = \frac{H_e \Phi_0}{2\pi} \sum_{i=1}^{2N-1} (\varphi_i - \varphi_{i+1}) \\ &= \frac{H_e \Phi_0}{2\pi} (\varphi_1 - \varphi_{2N}). \end{aligned}$$

We will treat value G as a height (or potential energy) of a mountain relief on multidimensional set of coordinates. Configurations, settled at some value of the external field h , correspond to the minimums of energy (hollows) in this relief. If h abruptly increases by some small value, this will result in some modification of the relief, after which the configuration (set of coordinates), corresponded to the minimum of the previous relief, will find itself on the hillside of the new one. The further change of this configuration shape can be considered as „rolling down“ the new relief with decrease of „potential energy“. Let's assume that this process happens as a result of large amount of small steps. It is logically to assume, that in each „point“ the rolling is performed along the line of the steepest descent, i.e. along the gradient of function G . This means that with each step all „coordinates“ of φ_i get increments, proportional to the corresponding gradient projection:

$$\Delta\varphi_i = -\frac{\partial G}{\partial\varphi_i} \delta,$$

where δ is low constant multiplier, setting the step value. Then, we calculate all $\partial G/\partial\varphi_i$ in the new point, i.e. at new values of φ_i , and make the next step. This procedure is repeated until we get the new stable configuration, located in relief hollow, corresponding to the specified h .

From (2) we get the expressions for „gradient projections“ of G :

$$\frac{\partial G}{\partial\varphi_i} = 2\varphi_i - \varphi_{i-1} - \varphi_{i+1} + g \sin \varphi_i, \quad (2 \leq i \leq 2N-1), \quad (3a)$$

$$\frac{\partial G}{\partial\varphi_1} = \varphi_1 - \varphi_2 + g \sin \varphi_1 - 2\pi h, \quad (3b)$$

$$\frac{\partial G}{\partial\varphi_{2N}} = \varphi_{2N} - \varphi_{2N-1} + g \sin \varphi_{2N} + 2\pi h. \quad (3c)$$

In [10,11] the point at the boundary of the Meissner mode H_S was selected as an initial point for this algorithm. This method allows to calculate the Meissner configuration from only near one contact end, i.e. on the assumption of the contact infinite length. In the examined situation the contact length is finite, therefore other end should also be considered. Distribution of φ_i corresponds to the minimum of the Gibbs potential, therefore it can be calculated, using the same method as for $h > h_S$ in [11].

This approach is also preferable for the infinite length contact [10], because, firstly, for all field values the single calculation method is applied, and, secondly, it gives the more accurate result. In the method, applied earlier [10], the value of φ_1 was specified and the possible value of φ_2

was found, at which there is a solution in the form of monotonously reduced combination of values of φ_m with m increase. But change of φ_2 significantly influenced φ_m for not very high numbers $m < M$. At the same time, the calculated value of φ_m had an order of at least 10^{-8} , while all φ_m at $m > M$ were equal to zero. But in reality they should be nonzero. The new approach allows to calculate all φ_m until the values of order of 10^{-15} , that allows to obtain the more accurate results.

We select the field value $h = 0$ as the initial point, while all φ_i are equal to zero. Let's give h some small increment for Δh and provide opportunity for „the point“ to move along „the line of the steepest descent“, as was explained above. In terms of programming this means to set a cycle, on each step of which the new values of φ_m at $1 \leq m \leq 2N$ are calculated as per formula $\varphi_m = \varphi_m - \frac{\partial G}{\partial\varphi_m} \delta$ considering (3). Finally, we get the configuration, in which all derivatives of $\partial G/\partial\varphi_i$ become zero. This is the desired equilibrium configuration, corresponding to $h = h_S + \Delta h$. Then, starting from this configuration, we can give a new increment for Δh , etc. This way we can find the distribution of currents and phase jumps at any value of the external magnetic field.

It should be noted, that the simplified calculation, that uses not gradual change of h from zero to the researched value of h_1 , but the direct setting of the value of h_1 from the start and the following application of above mentioned algorithm of Gibbs potential minimization, results in exactly the same values of φ_m . But it takes much less time.

At the second stage let's examine the change of situation with gradual increase of the transport current, passing through the contact in direction against us. The initial configuration will be the calculated at the first stage (at zero transport current) distribution of φ_m at $1 \leq m \leq 2N$. Let's set the low value of current j .

Then, the expressions for „gradient projections“ G from (3) are the following:

$$\frac{\partial G}{\partial\varphi_i} = 2\varphi_i - \varphi_{i-1} - \varphi_{i+1} + g \sin \varphi_i, \quad (2 \leq i \leq 2N-1), \quad (4a)$$

$$\frac{\partial G}{\partial\varphi_1} = \varphi_1 - \varphi_2 + g \sin \varphi_1 - 2\pi(h - j/2), \quad (4b)$$

$$\frac{\partial G}{\partial\varphi_{2N}} = \varphi_{2N} - \varphi_{2N-1} + g \sin \varphi_{2N} + 2\pi(h + j/2). \quad (4c)$$

Summing up the equations (4) for all i from 1 to $2N + 1$, we get

$$\sum_{i=1}^{2N} g \sin \varphi_i = j,$$

i.e. the sum of all currents is equal to j , as we thought from the beginning.

New values of φ_m are calculated as per formula $\varphi_m = \varphi_m - \frac{\partial G}{\partial\varphi_m} \delta$. Then, starting from this configuration, we can set the new current value, not much exceeding the previous one, and so on. Thus we can study the distribution of phase jumps φ_i , and hence of currents and magnetic

fields inside the contact in the whole range of the transport current change.

According to (2), normalized magnetic induction inside the m -th cell $b_m = \Phi_m/\Phi_0$ can be calculated as per formula

$$\varphi_m = (\varphi_{m+1} - \varphi_m)/2\pi.$$

2. Calculation results, their interpretation and analysis

Critical value of the pinning parameter g_C was determined in [12] and was equal to 0.9716. Let's examine the value $g < g_C$, particularly $g = 0.90$ ($h_S = 0.318$, $h_{max} = 0.344$).

Computer calculations completely confirmed the possibility of the proposed algorithm use for calculation of the field penetration into the contact. Indeed, by gradually increasing the value of the magnetic field from zero to h , and then by increasing the current from zero to j , it is possible to track the gradual change of the configuration, wherein at all values of h and j all $\partial G/\partial \varphi_i$ are equal to zero, i.e. G has the minimum. For each value of h there is a maximum current value, above which the stationary picture does not exist.

Figure 2 shows the diagram $j_C(h)$ of critical current dependence on the external magnetic field at $g = 0.9$ ($h_S = 0.318$) and contact length of 20 cells.

Let's examine the conditions, at which the vortices movement appears.

A) While $h + j/2 < h_S$, from both contact ends the Meissner configurations are built. If Meissner depth is considered low compared to the contact length, this range of current change is of no interest.

B) In case of $h_S < h + j/2 < h_{max}$ and $h_S < |h - j/2| < h_{max}$ the finite length structures will be from the both ends. If contact length is larger than these structures lengths sum, this situation remains stationary. If these structures overlap, the issue of stationarity needs to be studied.

Let's perform the analysis of the dependence of near-boundary structure length on the magnetic field for field h

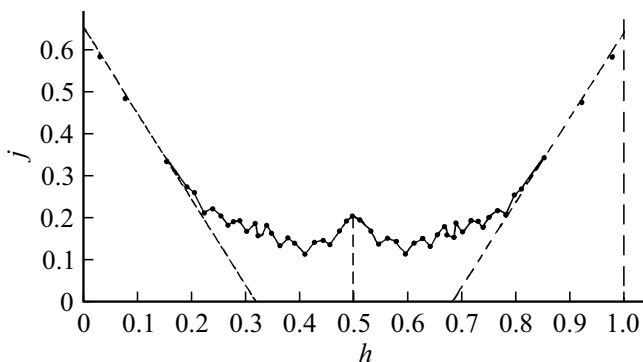


Figure 2. Dependence of the critical current on the external magnetic field at $g = 0.9$ and contact length of 20 cells.

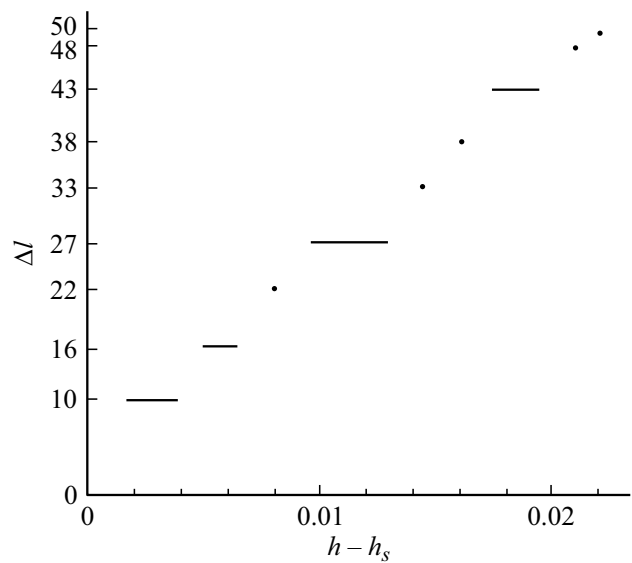


Figure 3. Dependence of the length of near-boundary vortex structure (in cells number) on the external magnetic field.

in a range of $h_S < h < h_{max}$. Let's calculate as per the above mentioned technique the values of the magnetic field in the cells $b_m = (\varphi_{m+1} - \varphi_m)/2\pi$ at various values of the field h for the contact with a length of 100 cells. Figure 3 shows the diagram of structure length (in cells number) dependence on the value of $h - h_S$.

Meeting the both conditions $h_S < h + j/2 < h_{max}$ and $h_S < j/2 - h < h_{max}$ is possible, if $h_S < j/2 < h_{max}$ and $h < \min\{j/2 - h_S, h_{max} - j/2\}$ at the same time. These ranges are rather narrow [11], but this situation is possible in principle. In this case the near-boundary vortex structures will be from the both sides, while their orientations will be opposite, since the field values from different sides from the contact have different signs. Therefore, if the contact length is less than these structures lengths sum, the vortices will annihilate each other in the area of their intersection. Vortices with opposite orientations will appear from both sides of the contact, move inward, to the place of „annihilation“, and disappear there. At vortices movement the energy will transfer to a heat and radiation, therefore the current will cease to be persistent.

C) If $h + j/2 > h_{max}$, the sequence of vortices will appear at the right end, trying to occupy the whole contact length. The left structure can be either Meissner configuration or finite near-boundary structure or vortices chain, also trying to occupy the whole contact. It may seem, that for the whole structure movement it is sufficient for the system to have vortices with the force applied to them. With any low current the field at the right end is bigger than at the left, the force is bigger on the right than on the left, and vortices should move from the right to the left. However, this is not true. It is sufficient to note that with the lack of the transport current the vortex structures are in the rest state, since the forces, acting on

the central vortex from the different sides, while exist, are equal to each other. When the current is not zero, one of the forces will be bigger than another, but movement will be prevented by the pinning on contact cells. For the movement to exist the force from one side should be bigger than from another by the value of the pinning force, i.e. the current should exceed some finite value. The detailed calculation is required to observe it. The proposed approach allows to perform it.

Analysis of the diagram of Fig. 2 allows to make the following conclusions:

1) Dependence $j_c(h)$ is periodical over the magnetic field h with a period of 1, that allows to extend it to other values of h . Periodicity arises from the fact, that with h increase by a unit, the system of equations (4) can be satisfied by means of increase of difference between any adjacent values of φ_i by 2π . It follows, that the maximum critical values of the transport current can be reached at the magnetic field h , equal to any integer of N .

2) Dependence $j_c(h)$ turns out almost strictly symmetrical relating to $h = 0.5$. It would seem, that it follows from the equations (4). By replacing the variable $\varphi_m = \xi_m - 2\pi n$ in (4) we get

$$\frac{\partial G}{\partial \xi_i} = 2\xi_i - \xi_{i-1} - \xi_{i+1} + g \sin \xi_i, \quad (2 \leq i \leq 2N-1), \quad (5a)$$

$$\frac{\partial G}{\partial \xi_1} = \xi_1 - \xi_2 + g \sin \xi_1 + 2\pi(1 - h + j/2), \quad (5b)$$

$$\frac{\partial G}{\partial \xi_{2N}} = \xi_{2N} - \xi_{2N-1} + g \sin \xi_{2N} - 2\pi(1 - h - j/2). \quad (5c)$$

It is easily seen that with numeration change in (5) to the opposite one the systems (4) and (5) are equivalent at h_1 and $h_2 = 1 - h_1$, i.e. there is a symmetry relating $h = 0.5$. However, this conclusion is wrong. Systems (4) and (5) have multiple solutions, therefore at h_1 and $h_2 = 1 - h_1$ various configurations can be set.

Initial (at $j = 0$) diagrams of the field distribution $b_m(m)$ in the contact for h and $1 - h$ are not identical, since the pinning does not allow configuration to track the value of the external field, that results in hysteresis. But at $j = j_c$ the configurations become identical. The reason is that at the established movement of the vortex picture in all cells the values of the fields, that minimize the Gibbs potential, will be set. As an example let's examine (Fig. 4) the dependencies of the normalized induction of the magnetic field $b_m = (\varphi_{m-1} - \varphi_m)/2\pi$ on the cell number m at $h = 0.204$, $j = j_c = 0.259$ and at $h = 0.796$, $j = j_c = 0.258$. The diagrams have a symmetry relating the point K , i.e. b_m from the first dependence corresponds to $1 - b_{20-m}$ from the second. This correspondence confirms and explains the symmetry of the dependence $j_c(h)$ relating $h = 0.5$ in Fig. 2.

3) Let's examine the nature of the performed processes depending on the value of the external field h .

At $h < h_s = 0.318$ by the beginning of the second stage of calculation ($j = 0$) at both ends of the contact

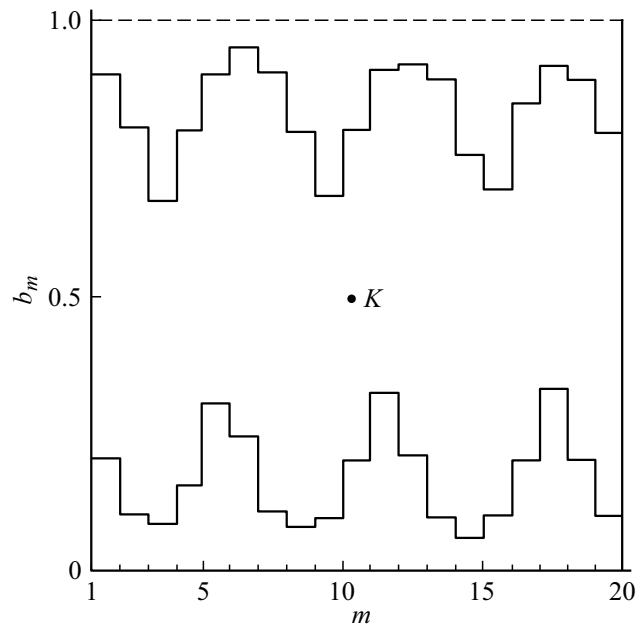


Figure 4. Dependencies of the normalized induction of the magnetic field b_m on the cell number m at $h = 0.204$, $j = j_c = 0.259$ and at $h = 0.796$, $j = j_c = 0.258$.

the Meissner configurations appear, without vortices. If current is supplied at, the right end near which the field is equal to $h + j/2 > h_s$, the vortex structure appears, at the left end the field is equal to $h - j/2 < h_s$, i.e. no vortices. For the vortex structure to reach the left end, the field should be equal to $h_s + \Delta$, where value of Δ depends on contact length and can be defined from Fig. 3. It would seem, that the condition of vortices movement has the form of $j/2 = h_s + \Delta - h$. With contact length of 20 cells from Fig. 3 we find $\Delta \approx 0.008$. In Fig. 2 the dashed line corresponds to ratio $j = 2(0.318 + 0.008) - 2h = 0.652 - 2h$. However, at small contact lengths this consistency is violated. The reason is in the influence of the Meissner configuration on the left: it can either prevent from movement (with the same orientation as vortices on the right) or contribute to it (with the opposite orientation). Lack of Meissner configuration on the left corresponds to zero field at the left end of the contact $h - j/2 = 0$, and from condition $h + j/2 > h_s$ we get $h = j/2 \approx h_s/2 = 0.159$. Indeed, in this point the diagram intersects with the line.

Left from this point, at $h < h_s/2$, we have $j/2 = h_s + \Delta - h > h_s/2$, i.e. the field at the left end of the contact ($h - j/2$) is negative, and the Meissner configuration, set there, has the opposite orientation. In this case the vortices movement starts, when the right configuration reaches the left Meissner structure, not the edge of the contact, therefore $\Delta < 0.008$, critical current is less than observed as per formula $j = 0.652 - 2h$, and points on diagram of Fig. 2 are below the line $j = 0.652 - 2h$. Value of this reduction is small.

At $h_S/2 < h < h_S$ the Meissner configuration of the same orientation appears at the left end, and it resists to the vortices chain movement from the right to the left. Therefore, the points are above the line.

Such situation happens, for instance, at $h = 0.240$, when $j_C/2 = 0.110$, $h + j_C/2 = 0.350$, i.e. $h_P = 0.006$ is a resistance to the vortices movement, created with the Meissner configuration at $h - j_C/2 = 0.130$. At $h = 0.310$ we have $j_C/2 = 0.082$, $h + j_C/2 = 0.392$, i.e. $h_P = 0.048$. Such resistance is created with the Meissner configuration, corresponding to $h - j_C/2 = 0.228$. The larger „the height“ of the Meissner configuration, the bigger is resistance.

At $h > h_S$ at the left end the vortex configuration appears from the beginning (at $j = 0$). With increase of the current j the field to the left from the contact, equal to $h - j/2$, reduces, but due to the pinning the vortices continue to exist even at $h - j/2 < h_S$. Figure 2 shows that at $h > h_S$ the condition $h > j_C/2$ is met. Therefore, until the critical current the structures at different ends are oriented identically, so there is no annihilation. But since the field at the right end is bigger than at the left end, the right structure displaces the left one from the contact, after which the situation is established, when vortices appear at the right boundary of the contact, move to the left and disappear at the left end.

It is logical to consider, that the moving force is proportional to the fields difference at the edges j . Figure 2 shows, that in a range from $h = 0.215$ to 0.785 the value of j_C varies between the values of 0.12 and 0.20 . It may be concluded that the resistance to the vortex chain movement with increase of h remains almost constant, while fluctuations are defined with details of vortices pinning on the cells.

It should be noted, that in the works [15,16] the influence of the current profile on volt-ampere characteristics and nature of the traveling wave in the external field presence was analytically and numerically studied. Particularly, in [16] the diagram of the field distribution inside the contact is presented, but for another discontinuity type.

Conclusion

The possible distributions of currents and magnetic fields inside the long periodical ordered Josephson contact, put into the external magnetic field and through which the transport current is passed, are calculated. The case is examined, when the pinning parameter is less than critical ($g < g_C$). For calculation the approach based on analysis of continuous modification of configuration, going in direction of the Gibbs potential decrease, is used.

It is shown, that at any value of the external magnetic field there is a critical value of the transport current, at exceeding of which the situation ceases to be stationary, resulting in the energy transition into radiation and heat, i.e. currents cease to be persistent.

The detailed analysis of the performed processes is carried out, providing the qualitative explanation of the observed consistencies.

In case of $g < g_C$ the critical current is defined with the value of the magnetic field H_{max} , at which the vortices start to occupy the whole contact length, and does not depend on contact length. When putting the contact into the external magnetic field, the value of the critical current decreases.

Dependence of the critical current on the external magnetic field is periodical over the magnetic field h with a period of 1, that allows to extend it to other values of h . Therefore, the maximum critical values of the transport current can be reached at the magnetic field h , equal to any integer of N .

Conflict of interest

The author declares that he has no conflict of interest.

References

- [1] A.P. Drozdov, P.P. Kong, V.S. Minkov, S.P. Besedin, M.A. Kuzovnikov, S. Mozaffari, L. Balicas, F.F. Balakirev, D.E. Graf, V.B. Prakapenka, E. Greenberg, D.A. Knyazev, M. Tkacz, M.I. Eremets. *Nature*, **569**, 528 (2019). DOI: 10.1038/c41586-019-1201-8
- [2] M. Somayazulu, M. Ahart, A.K. Mishra, Z.M. Geballe, M. Baldini, Y. Meng, V.V. Struzhkin, R.J. Hemley. *Phys. Rev. Lett.*, **122**, 027001 (2019). DOI: 10.1103/PhysRevLett.122.027001
- [3] A.A. Golubov, I.L. Serpuchenko, A.V. Ustinov. *Sov. Phys. JETP*, **67**, 1256 (1988).
- [4] L.S. Revin, A.L. Pankratov, D.V. Masterov, S.A. Pavlov, A.V. Chiginev, E.V. Skorokhodov. *IEEE Transactions Appl. Superconductivity*, **28** (7), 1100505 (2018). DOI: 10.1109/TASC.2018.2844354
- [5] B. Chesca, D. John, C.J. Mellor. *Supercond. Sci. Technol.*, **27**, 085015 (2014). DOI: 10.1088/0953-2048/27/8/085015
- [6] I.A. Golovchanskiy, N.N. Abramov, V.S. Stolyarov, O.V. Emelyanova, A.A. Golubov, A.V. Ustinov, V.V. Ryzanov. *Supercond. Sci. Technol.*, **30** (5), 054005 (2017). DOI: 10.1088/1361-6668/aa66a9
- [7] L.S. Revin, A.L. Pankratov, A.V. Chiginev, D.V. Masterov, A.E. Parafin, S.A. Pavlov. *Supercond. Sci. Technol.*, **31** (4), 045002 (2018). DOI: 10.1088/1361-6668/aaacc3
- [8] E.M. Rudenko, I.V. Korotash, A.O. Krakovnyy, M.O. Bilogolovskyy. *Metallofiz. Noveishie Tekhnol.*, **40** (10), 1273 (2018). DOI: 10.15407/mfint.40.10.1273
- [9] M. Nashaat, A.T. Botha, Yu.M. Shukrunov. *Phys. Rev. B*, **97** (22), 224514 (2018). DOI: 10.1103/PhysRevB.97.224514
- [10] M.A. Zelikman. *Supercond. Sci. Technol.*, **12** (1), 1 (1999).
- [11] M.A. Zelikman. *Tech. Phys.*, **54** (12), 1742 (2009). DOI: 10.1134/S1063784209120044
- [12] S.N. Dorogovtzev, A.N. Samuhin. *Europhys. Lett.*, **25** (9), 693 (1994).

- [13] G.M. Zaslavskij, R.Z. Sagdeev. *Vvedenie v nelinejnyu fiziku* (Nauka, M., 1988) (in Russian).
- [14] M.A. Zelikman. *Tech. Phys.*, **66** (8), 1178 (2021).
DOI: 10.1134/S1063784221080181
- [15] A.I. Pankratov. *Phys. Rev. B*, **66**, 134526 (2002).
DOI: 10.1103/PhysRevB.66.134526]
- [16] E.A. Matrozova, A.L. Pankratov, L.S. Revin. *J. Appl. Phys.*, **112**, 053905 (2012). DOI: 10.1063/1.47481511.